Chapter 6
Putting Nanoparticles to Work: Self-propelled Inorganic Micro- and Nanomotors

Kaitlin J. Coopersmith

Abstract The development of nanomotors (nano- and micron sized particles that convert energy into mechanical movement) is an exciting endeavor. Nanomotors have been crafted in an extensive variety of sizes, morphologies and compositions for applications such as drug delivery, cargo transport, sensing, and lithography. Inspired by nature's elegant use of chemical gradients and cellular tracks for independently driven molecular processes, a variety of machines have been created. With the recent bestowment of the Nobel Prize for molecular machines, this concept is being actively pursued to create inorganic nano- and microparticles that independently move for a gamut of applications.

Keywords Anisotropic nanoparticle · Bimetallic nanoparticle · Nanomotor · Micromotor · Propulsion · Autonomous movement · Sensing · Acoustic · Optical · Magnetic · Electrophoresis · Biofuel

6.1 Introduction

As technological creations become smaller, machines that perform work expand into the micro- and nano-sized regimes. With the advancement of nanotechnology, the creation of nanoscopic machinery is becoming a popular endeavor. Molecular machines have been crafted using various molecules that interact with light, sound, and biological entities to create miniscule moving parts that are highly controlled [1–3]. More recently, nanomotors have been fabricated from micro- and nanoparticles rather than molecules [4–10]. This exploits the unique optical and physical properties of micro and nanoparticles that are highly dependent on size, composition, and morphology. Typically, nanomotors do not have moving parts, although, carbon nanotube based machines with moving parts have been created [9].

K.J. Coopersmith (✉)
National Security Directorate, Savannah River National Laboratory, Aiken, SC, USA
e-mail: kaitlin.lawrence@srnl.doe.gov

S.E. Hunyadi Murph et al. (eds.), *Anisotropic and Shape-Selective Nanomaterials*,
Nanostructure Science and Technology, DOI 10.1007/978-3-319-59662-4_6

Nanomotors harvest energy from different forms of chemical or physical stimuli, including acoustic, optical, magnetic, and electrical energies and convert it into mechanical work [4–9]. Self-propelled nanoparticles have an array of applications related to medical treatment and diagnostics [4], biological and chemical sensing [7], energy storage [11], lithography [12], mass transportation [13, 14], and chemical degradation [15]. Self-powered nanomachines can cause controlled agitation without external energy, which can be useful in applications such as chemical degradation in ecosystems, where external agitation is not feasible but mixing is highly desirable. Compared to the diffusion controlled counterparts, nanomotors have higher reactivity due to the increased fluid transport [15]. The successful integration of nanomotors requires highly efficient propulsion using fuel at concentrations relevant to the applications. A variety of motors exists but with low efficiencies and high fuel concentration requirements that are not suitable for most biological applications. Propulsion speed is typically expressed in body lengths per second (bl/s), with speeds up to 176 bl/s having been reported for biological motors [16], 75 bl/s for inorganic nanomotors [8], and 375 bl/s for microtube nanomotors [17]. For comparison, a cheetah can only move with a speed of about 32 bl/s [18] and the record for the world's fastest land animal currently belongs to the *Paratarsotomus macropalpis*, a mite found in California that moves with a speed of 192 bl/s [19].

The sophistication found in biological entities have inspired the creation of nanomotors [20, 21]. Cells have an internal structure that is anisotropic and non-homogeneous and their complex makeup leads to directional flow and transport of materials [20]. Various molecular motors inside of the cells carry out the directional processes that overcome Brownian motion using stored chemical energy [20]. Flagella, which are tubular protein appendages, are present on most prokaryotic and some eukaryotic cells and move in response to ion gradients [22–24]. In prokaryotic cells, flagella move in sinusoidal wave-like motions and in eukaryotic cells, they move in whipping motions. Bacterial flagella are driven by a protein rotary engine that is powered by a proton gradient that comes about during the cell's metabolism [20]. Fig. 6.1i shows video micrographs of flagellar movement that resulted from the oscillatory sliding motion in bull sperm flagella in the presence of ATP and Ca^{2+} ions [24]. Transverse movement was attributed to the two sliding mechanisms that occur between adjacent double microtubules [24].

Cellular motor proteins can also move along a track. For example, dynein and kinesin convert energy from adenosine triphosphate (ATP) to movement along cytoskeletal tracks to generate forces and transport cargos (Fig. 6.1ii) [21]. Kinesin moves along a predefined path composed of microtubule (MT) filaments toward the positive end to transport cellular cargo as well as help the cell carry out mitosis and meiosis. Dyneins move along the MT's negative end to transport cellular cargo, position organelles in the cell, and play a role in other important cellular functions [21]. A more sophisticated biological motor is ATP synthase, the enzyme that produces ATP. It is made up of two rotary molecular motors that move in opposite directions depending on cell conditions [20].

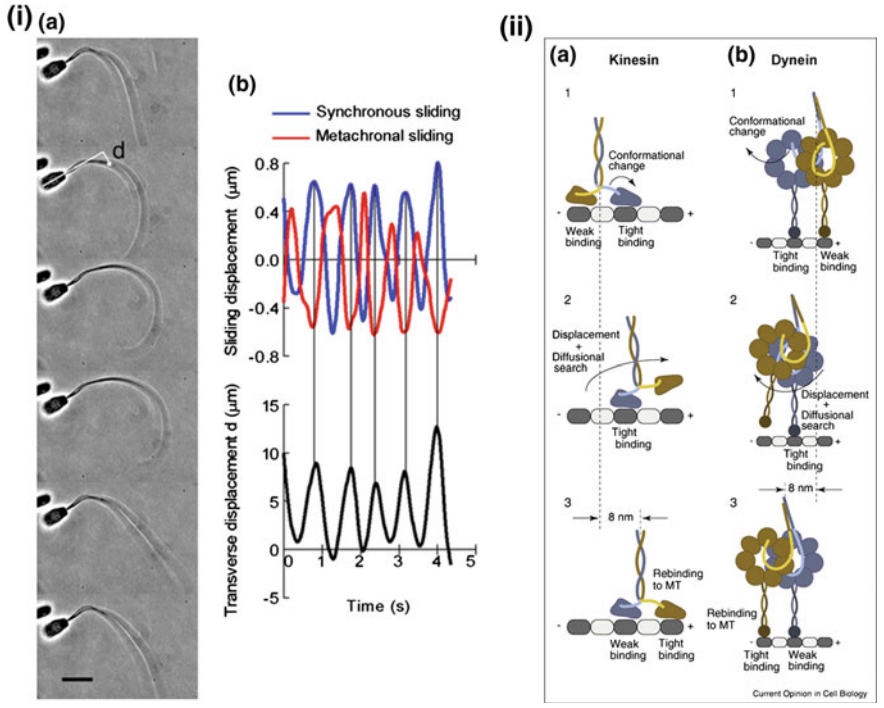

Fig. 6.1 Movement of biological motors: **i** (*a*) Phase contrast micrograph of the effect of sliding displacement on transverse displacement in bull sperm models (time interval between successive images t = 0.15 s; beat frequency of flagellar bending was f = 1.2 Hz); (*b*) profiles of microtubule sliding displacement and of the transverse displacement of the flagellum shown in (*a*). Scale bar = 10 μm. Open access from Ref. [24]. **ii** Models for (*a*) kinesin and (*b*) dynein stepping. Reprinted with permission from Ref. [23]

Nanomotors have been created from organic compounds, biological molecules such as DNA and enzymes, carbon nanoparticles, metals, metal oxides, and semiconducting materials, both with and without moving parts [4–10]. The altered movement of nanomotors in response to changes in the local environment can be exploited for chemical sensing, environmental remediation, electronic self-repair, among others [4–7]. In medical applications, nanomotors can be used to pick up and deliver chemical payloads or as intracellular gene silencers in genetic therapy [25]. Most of these applications focus on the creation of non-toxic and environmentally friendly nano- and micromotors. The speed, direction of movement, and trajectory is directly related to the concentration of fuel, which can be acoustic, optical, magnetic, electrophoretic/electrocatalytic, chemical, and enzymatic/catalytic. Movement can be varied with the addition of fuel, namely ions or secondary moieties/molecules/components, to the nanomotors. The speed can be dramatically increased or decreased when a combination of fuels are used [7]. For environmental or biological

applications, nanomotors are employed in complex sample matrices (e.g. high ionic strength), so high selectivity is imperative.

In liquid suspensions, the solvent's viscosity and the particle's drag force in the solvent have profound effects on motor movement. Locomotion in fluids is typically described by Reynolds number, which is the ratio of inertial forces to viscous forces. Due to their small sizes, the movement of nano- and micromotors takes place at low Reynolds numbers where viscous forces dominate [26]. Since inertial forces do not play a role, motors in this regime must continuously apply force to move. Particle diffusion can be understood using Stokes' Law, which calculates the drag force experienced by a spherical particle with a certain radius in low Reynolds' number regimes. Diffusion coefficients are also size dependent, so it is harder for smaller motors to move in response to a field. Nanomotors have to overcome hydrodynamic forces (e.g. diffusion and viscous drag), Brownian motion and rotation, and unfavorable interactions with the energy source (e.g. magnetic or plasmonic heating) or physical environment. Non-equilibrium forces are required to create directional movement. Thus, careful design of the nanomotor and power source must be carried out to ensure the movement is related to the power source rather than hydrodynamic forces and Brownian motion. The interactions between the motors, such as repulsive or attractive forces or long-range ion gradients, can lead to assemblies and collective interactions that will also affect the movement of the motors [27]. Depending on the morphology, composition, and fuel used, the nano- and micromotors can have oscillatory or linear motion.

This chapter focuses on metallic inorganic nanomotors. These nanomotors are not typically made up of moving parts but rather are created in a way to facilitate movement through their anisotropic structure [7]. The biomimetic capabilities of nanomotors have also been applied to electronic applications, where nanomotors were used to autonomously seek and repair nano-and micro-sized cracks [6]. The ability to repair damage based on changes in the chemical or physical environment can be extended into the medical field, where nanomotors can be applied to help "heal" damage to the body. The ability of nanomotors to change speed and trajectory in the presence of certain chemicals is beneficial in a wide array of applications including chemical sensing and transport.

6.2 Synthetic Nanomotor Design

6.2.1 Synthesis and Characterization

A variety of approaches have been used to fabricate a wide array of nanomotors, including Janus particles, anisotropically shaped nanoparticles, and protein and polymer based particles. The movement of nano and micromotors in solution is typically tracked through optical spectroscopy. Videos and time lapse images are obtained and single particle tracking statistics are used to determine the speed and

trajectory of the motors [5, 7, 11]. Temporal particle tracks are used to graphically demonstrate the motor's trajectory [11]. Diffusion coefficients, which are typically on the order of $\sim 1\ \mu m^2/s$ for nanomotors, can be calculated from the slope from mean squared displacement plots or extrapolated from dynamic light scattering (DLS) measurements [28, 29]. Diffusion coefficients are used to quantify the mobility of the motors and are dependent on viscosity. Optical tweezers have also been used to measure the force required for propulsion [29].

The presence of ligands on nanomotor's surfaces will affect the movement and efficiency of the nanomotor, either hindering or enhancing the movement [30]. When ligands hinder the movement, anisotropic rods and wires can be synthesized without surface capping molecules via physical routes such as sequential electrodeposition onto templates [7, 10, 11, 30] or thermal evaporation [5]. In electrodeposition routes, the rod or wire length can be tuned via electrodeposition time where a longer deposition time leads to longer rods or wires. The fast movements of propelled nanomotors may also lead to a decrease in physically adsorbed species that can interfere with the movement or reactivity.

Anisotropy can be appended to particles that may not otherwise be anisotropic, such as spherical particles. For example, Janus nanoparticles have two or more domains with distinct physical or chemical properties. The different domains are typically fabricated by creating a separate domain on a spherical nanoparticle at various types of interfaces, such as air-liquid, liquid-liquid or gas-liquid interfaces. In the most common approach, nanoparticles are deposited onto substrates and the exposed side is coated with a different composition, either through wet chemistry [31], electron beam deposition [29] or altered sputtering processes [15]. In the thermal evaporation technique, single composition nanoparticles are attached to a substrate and metal vapor condenses onto the substrate in a vacuum, leading to the creation of a sphere with two different metallic domains [5]. Other synthetic methods, including the Kirkendall effect, may also be utilized to create anisotropic nanoparticles. For the Kirkendall effect, particles are synthesized from two incompatible metals that phase separate into individual domains. The ideal technique for nanomotor fabrication depends on the nanomotor's requirements.

6.2.2 Efficiency

Nanomotor efficiency is based on the conversion of fuel into mechanical motion. A variety of mechanisms contribute to efficiency loss, including consumption of the motor, depletion of the fuel, and side reactions, such as the decomposition of the fuel via paths that do not lead to movement [10, 11, 30]. Nanomotors should be able to be employed in complex sample matrices, where contaminants may be present. Various routes have been studied to increase the efficiency, including the photochemical decomposition to regenerate the nanomotor and fuel [30]. The efficiency is typically calculated using Eq. 6.1:

$$\eta = \frac{power\ output}{total\ power\ output}, \tag{6.1}$$

where η is the efficiency of the nanomotor as a function of power output (speed and trajectory) and total power input (chemical concentrations, etc.) [30]. The efficiency of nanomotors have been reported on the order of 10^{-9}–10^{-5}, and external field driven motors typically have higher efficiency than chemically driven motors [30].

6.3 Propulsion Routes

Synthetic nanomotors can be powered non-autonomously by external fields, such as magnetic [12, 13, 32–35], acoustic [25, 36–40], and optical [41–44] energies, or autonomously through self-generated chemical gradients [7, 11, 28, 45] or bubble propulsion [4, 15]. For motors powered via external fields, the speed and directionality may be easier to control. In contrast, chemically powered nanomotors do not require direct manipulation but they typically require high concentrations of chemicals, since the instantaneous efficiency depends on the amount of fuel remaining in solution. Chemically powered motors also have fine-tuned sensing capabilities, where movement as a response to changes in the environment can translate into lower detection limits and energy conservation for industrial applications such as water detoxification. The propulsion route and nanomotor design can be tailored depending on the desired application.

6.3.1 External Propulsion

External energy can be transduced into movement via magnetic, acoustic or optical energy, with speed and efficiency related to the strength and power of the energy input. These energy routes are non-contact and highly targeted methods that do not require additional chemical changes to the environment. External manipulation and control also gives one the ability to tune the route and location of the nanomotors with longer motor lifetimes.

6.3.1.1 Acoustic

Acoustic energy has been developed for medical treatment and diagnostics, such as ultrasonography. Due to the minimal adverse side effects on biological systems, the use of acoustic energy to power nanomotors for biologically relevant applications is desired. Nanorods, nanowires, and microrods have been accelerated in megahertz (MHz) acoustic fields without the addition of chemical fuel [25, 37–40]. In these

studies, standing waves are used to acoustically confine particles to a levitation plane, where the acoustic pressure is at a minimum (nodal plane). Experimental geometry can also be tailored to create arrays of particles. In the presence of acoustic radiation, spherical particles create linearly and spherically assembled shapes that are difficult to control [38]. Though anisotropic metal rods also displayed linear and spherical assembly, they displayed directional motion, in-plane rotation and pattern formations, as shown in Fig. 6.2 [38]. The directional motion was dependent on their location in the levitation plane and the frequency and the speed of the rods were tuned by changing the amplitude of the acoustic fields [38].

The mechanism that is believed to be responsible for movement in acoustic fields is the acoustic streaming mechanism, where particles oscillate in the plane of the acoustic field and experience a stress that causes them to move [37]. Particle asymmetry causes streaming effects that create a net force along the axis of the rods,

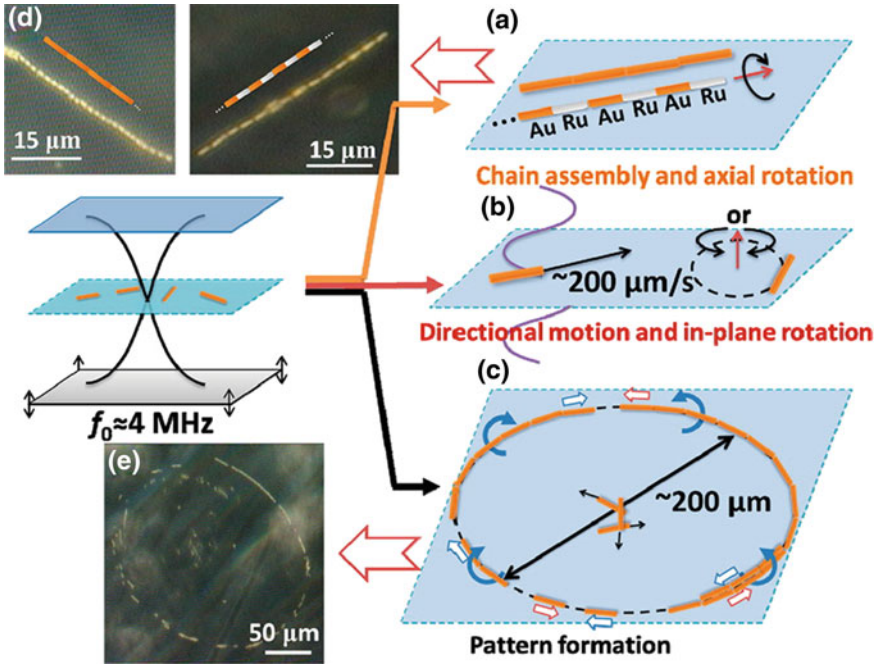

Fig. 6.2 **a–c** Illustration of the kinds of motion (axial directional motion, in-plane rotation, chain assembly and axial spinning and pattern formation, especially ring patterns) of metal microrods in a 3.7 MHz acoustic field. AuRu rods (gold-silvery color in dark field) showed similar behaviour to the Au rods, except that they moved with their Ru ends (the silvery end in the image) forward and aligned head-to-tail into chains. **d** and **e** Dark field images of typical chain structures and ring patterns formed by Au and AuRu rods. Note that the cartoons superimposed on **d** are intended to show the alignment of the rods and are not to scale or in proportion to the aspect ratio of the Au or AuRu rods. Reproduced with permission from Ref. [38] Copyright © 2012 American Chemical Society

leading to directional movement [37, 38]. For bimetallic nanorods, lighter density material led the movement of the nanomotor but when the materials had similar densities, the movement occurred in the direction of the concave end of the rod as opposed to the convex end due to shape asymmetry rather than material asymmetry [37].

Both cells and nanomotors can be manipulated using acoustic fields. When exposed to ultrasonic radiation, cells aggregate at pressure nodes that are perpendicular to the direction of the acoustic waves without damage to the cells or drug loaded nanomotors [46]. Acoustic fields can be used to increase the contact between cells and drug loaded nanomotors that can subsequently deliver their drugs [25, 46]. Enhanced propulsion under the influence of the acoustic field allows nanomotors to pierce through the cell membrane [25]. Drug therapy has been found to be more efficient in the presence of acoustic radiation [25]. More efficient drug therapy leads to lower drug concentration requirements, which can decrease the prevalence of unwanted side effects.

6.3.1.2 Optical

The first examples of nanomachines were created from organic molecules that change based on photochemical processes, such as photochemical cis-trans isomerization and thermal isomerization [47, 48]. When exposed to ultraviolet (UV) light, organic molecular motors rotate in response to the change in chirality. When the UV light is removed, the molecular motors rotate in the opposite direction due to thermal isomerization as the molecule relaxes back to the original structure. Organic molecular motors have been created that can rotate objects that are on the order of 10,000 times larger than their size when exposed to ultraviolet light [48]. Molecular motors have a large electronic effect that determines the rate of isomerization and the speed of rotation [47]. Alternatively, nanomotors based on inorganic nano and micron sized particles have been created from materials that interact with light, such as metal nanoparticles that have a surface plasmon band [41–44]. The optical torque of anisotropic gold nanostructures using light has been studied theoretically [41, 42] and experimentally [44]. Generally, the optical torque and direction depends on the polarization of the light, location of the surface plasmon resonance band, the efficiency of light absorption, solution viscosity, and magnitude of the light torque [41].

Figure 6.3 shows the interactions between AuNRs and circularly polarized light as well as the effect of torque on wavelength. At the surface plasmon resonance band, rotational torque is at a maximum; however, no rotation was observed with linearly polarized light [41]. Nanomotors that rotate in response to light can be used as nano stir bars or as probes measure biological processes or determine the viscosity of nano environments [44].

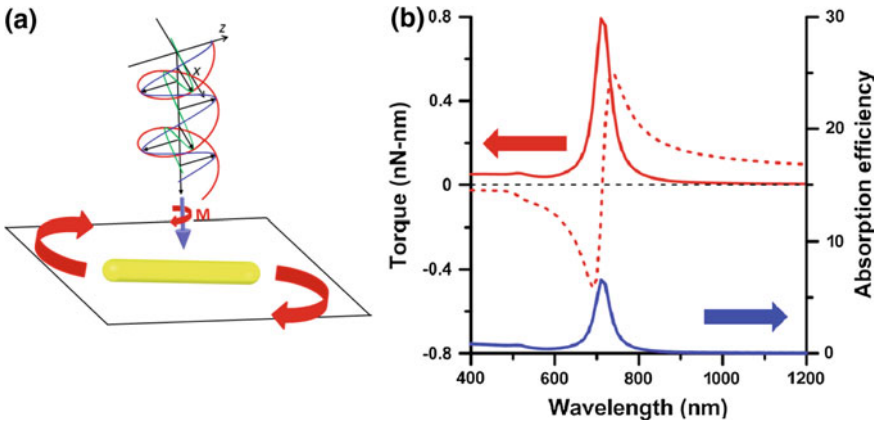

Fig. 6.3 **a** AuNR rotation as a response to circularly polarized light; **b** effect of absorption efficiency on torque for a rotating AuNR. Open access from Ref. [41]

6.3.1.3 Magnetic

Another external actuation mechanism involves the use of magnetic fields [12, 13, 32–35]. Propulsion has been achieved using homogenous rotating magnetic fields and magnetic field gradients, though as the size of the nanomotor decreases, actuation by the former becomes more reliable [12, 33]. Magnetically propelled machines typically contain helical or chiral components that allow them to be steered through a matrix. Independent control over propulsion in a mixture of different nano and micromotors has been achieved in a variety of different ways [12, 33]. In one route, two different nanomotors can be combined that respond to different types of magnetic fields. Alternatively, various nanomotors can be fabricated with different magnetic moments or speed-frequency relationships [12, 33]. For the latter, the ratios between speeds of the different propellers are related to the ratios between the critical frequencies, allowing for predictable motor control [12]. Nanomotors propelled via magnetic fields have been used for assembly, material delivery, and nanomotor lithography. Magnetic manipulation is useful for biological applications because most biological systems can tolerate magnetic field energy. As a result of this benefit, magnetic nanomotors have been used for applications such as the magnetic delivery of drugs using a predetermined route [13], biosensing [49], among others.

6.3.2 Chemical Propulsion

Chemically powered motors use stored chemical energy as the power source, leading to a fully autonomous movement without the need for external energy.

In these systems, there is an imbalance in the chemical environment that drives the motion. Chemical mechanisms that have been used to describe nanomotor acceleration in the presence of fuel or ions include underpotential deposition (UPD), where ions are absorbed and reduced on the surface [7], self-generated ion gradients, catalyzed reactions, and gas propulsion as a result of gas release from chemical reactions. The speed and directionality of chemically powered nanomotors depends on the nano-engineered motor as well as the amount of the fuel.

6.3.2.1 Diffusiophoresis

Movement can result from a gradient of uncharged solutes (electrophoretic movement) or a gradient of charged solutes (chemophoretic movement) on motor's surfaces [7, 11, 28, 45]. These mechanisms direct movement in particles by creating a gradient of particles that generates a change in osmotic pressure, leading to fluid flow in the direction of higher concentrations of ions or chemicals [28]. In self-electrophoresis, or the movement in the presence of a self-generated ion gradient, the change in ion concentrations results in movement via electro-osmotic flow through the change in the electrical double layer. Since the movement is dependent on ion concentrations, speed typically decreases with solution conductivity [7]. Nanoparticles that are propelled by self-generated chemical concentration gradients are propelled by self-diffusiophoresis and are effective even in high ionic conditions; however, these nanomotors tend to have slower speeds compared to electrophoretic conditions [27]. The fastest diffusiophoretic mechanisms occur in systems that release protons since the diffusion of protons is an order of magnitude faster than the diffusion of anions [27].

One of the most well studied self-electrophoretic fuel mechanisms is the decomposition of H_2O_2 in the presence of bimetallic rods and wires [7]. In one example, Au–Pt nanowires were used, where the Pt–Ag system acted as an anode–cathode for the decomposition of hydrogen peroxide. This system had an unusual increase in speed with an increase in solution conductivity when the added ion was Ag^+. In the presence of Ag^+ ions, there was a dramatic increase in speed, from 10 μm s^{-1} to 52 μm s^{-1}, whereas the addition of other metal ions led to a decrease in speed, ranging from 0.3 to 7.1 μm s^{-1} [7]. This increase in speed was attributed to underpotential deposition (UPD), where the Ag was reduced at the Pt surface of the nanowires, leading to Au–Pt–Ag compositions. Control experiments indicated that the acceleration was due to the addition of the Ag domain. This added domain possibly led to an increased difference in chemical potentials between the anode and the cathode, an increase in the catalytic activity, and an increase in concentration gradient of reaction products around the rod (self-diffusiophoresis).

Although hydrogen peroxide is one of the more well studied fuels, other materials such as halogen liquids have been investigated. Figure 6.4 shows an example of a bimetallic nanowire that moved in response to the addition of Br_2 and

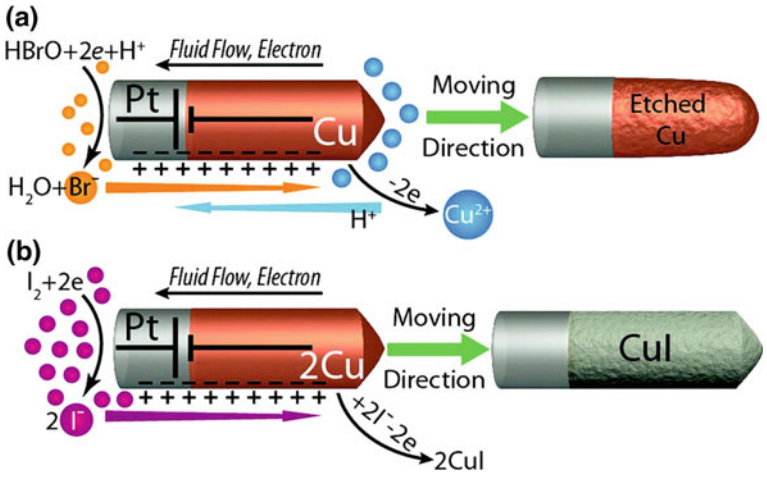

Fig. 6.4 Effect of aqueous solutions of Br_2 (a) and I_2 (b) on Cu morphology in Pt–Cu bimetallic nanowires. Reproduced with permission from Ref. [11]. Copyright © 2012 American Chemical Society

I_2 solutions due to the etching of the Cu domain in Br_2 and the conversion of Cu to CuI in I_2 solutions [11]. The movement of the nanowire is in the opposite direction of the fluid flow. The shorter the Cu segment, the faster the rods moved but the shorter the lifetime due to the consumption of the Cu metal [11].

In this study, asymmetric Cu nanorods were also synthesized into a ratchet shape and introduced into I_2 to create a rotor. The different redox reaction rates at the anisotropic end of the Cu nanorod led to the torque for the rotational movement [11].

Enzyme catalytic reactions are specific and efficient reactions that can occur even in the highly molecularly crowded locations inside of cells [50]. There is a large library of known enzymatic reactions, with over 2000 known enzymes. Since enzymes are found in living cells, they have a high biocompatibility that is beneficial for in vivo cargo delivery, biological sensing and other biomedical applications [29, 50]. In one example, Janus nanoparticles were created and functionalized with three different enzymes as shown in Fig. 6.5 [29]. The enzyme functionalized nanoparticles had directional movement as a result of the chemical gradient from the enzyme catalyzed reactions [29]. An increase in diffusion coefficient was measured with increasing fuel concentrations up to a saturation point (Fig. 6.5c), which was attributed to the Michaelis-Menten enzyme kinetic values and the viscosity of the solution due to increased glucose fuel concentration. Unlike the H_2O_2 fueled motors, these motors used glucose and urea, which are biologically benign [29].

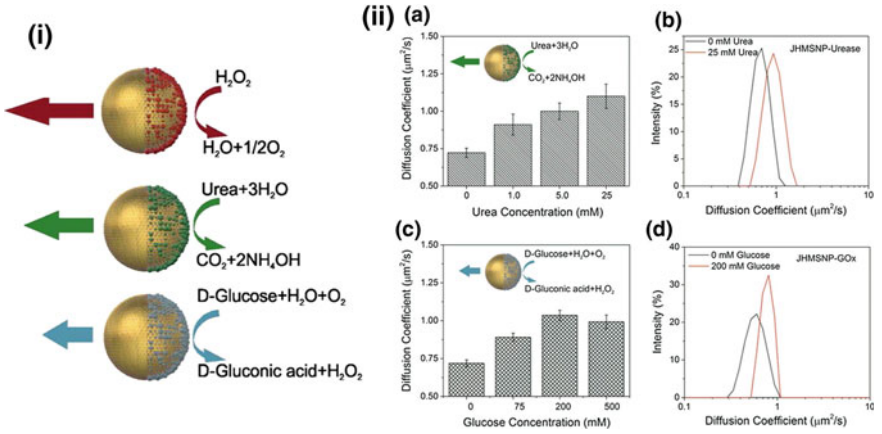

Fig. 6.5 **i** Overview of the different enzymes used to create self-propelled nanomotors. **ii** (*a*) Diffusion coefficient as a function of urea concentration for urease functionalized nanoparticles; (*b*) effect of urea on DLS measured diffusion coefficient; (*c*) diffusion coefficient as a function of glucose concentration for glucose oxidase functionalized nanoparticles. Open access from Ref. [29]

6.3.2.2 Bubble Propulsion

Micro- and nano sized jets have been created that are propelled via bubble recoil (Fig. 6.6). In these systems, bubbles are created due to a chemical reaction on one side of the nanomotor. For example, in the creation of H_2 gas from a metallic reaction with water or acid [15, 51], the hydrogen bubble thrust generated as a result of the reaction led to particle propulsion in the opposite direction. Controlled and gradual dissolution leads to an increase in nanomotor lifetime. This has been accomplished through various routes, including in core/shell architectures, where the presence of a small "hole" in the shell allows gradual exposure of the reactive species [15]. Bubble formation has also been used to create nanomachines that move in response to the ejection of single layer graphene sheets as a result of H_2 release from the sodium-water reaction [51].

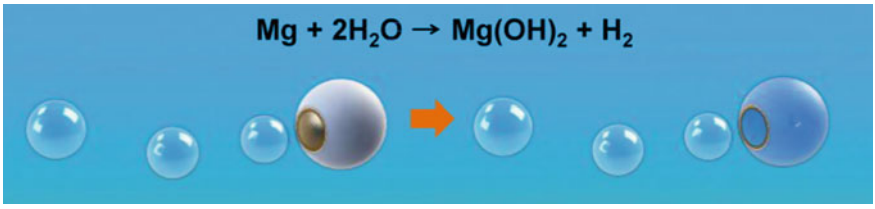

Fig. 6.6 Nanomotors powered via bubble propulsion as a result of the manganese reaction with water. Reproduced with permission from Ref. [15]. Copyright © 2014 American Chemical Society

6.3.3 Multiple Energy Sources

Dual-fuel and hybrid motors have also been realized for increased flexibility, control, and lifetime [5]. In one example, Ag/Mg Janus microparticles could be propelled in two directions based on the fuel; silver was propelled through electrocatalytic reactions with hydrogen peroxide and the magnesium component was propelled through the water–magnesium reaction with sodium bicarbonate as fuel. These nanomotors moved with an average velocity of 90 μm s^{-1} in sodium bicarbonate (~3.6 bl/s) and 67 μm s^{-1} in hydrogen peroxide (~2.7 bl/s) and traveled for 15 and 30 min in sodium bicarbonate and hydrogen peroxide, respectively, before consuming all of the fuel [5]. When exposed to *E. coli* with and without fuel, these motors killed 90% of the bacteria when the fuel was added, compared to 10% for the static motors. The more efficient antibacterial properties of the moving nanomotors was a result of the increased movement of the Janus particles in solution, allowing more bacteria to be exposed to the antimicrobial silver portion. These findings can lead to more efficient antimicrobial delivery and a decrease in antibiotic resistance.

Nanomotors that are powered by two different energy routes, also known as hybrid nanomotors, have been created [34–36]. These can be used to overcome the limitations of certain fuel sources or to reverse motion [36]. In one example, nanowires were created with Ag, Ni and Pt segments for catalytic and magnetic powered motors [34]. Individually, the motors experienced similar speeds in the presence of either catalytic fuel or magnetic energy; however, in the presence of both, the speeds were slower due to the increased fluid drag resistance from opposing propulsion forces [34].

Figure 6.7 shows the design of a hybrid nanomotor that can be powered using either acoustic or magnetic energy [35]. In these nanomotors, the concave Au nanorod segment responded to acoustic fields and the Ni coated Pd segment responded to a magnetic field. The magnetic propulsion was achieved using a rotating magnetic field with speeds of 12.2 μm/s and the acoustic propulsion, under an ultrasound field, led to speeds of 16.8 μm/s [35]. Creating nanomotors that can be powered using two different routes offers a new degree of flexibility for their use in dynamic environments [35].

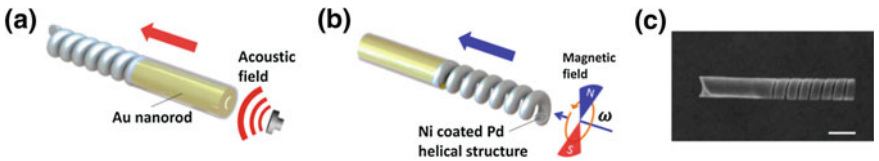

Fig. 6.7 Hybrid nanomotor that can be powered by **a** acoustic energy, which is absorbed by the Au nanorod segment, or **b** magnetic energy, which is absorbed by the Ni coated Pd segment; **c** SEM image of the magneto-acoustic nanomotor (scale bar = 500 nm). Reproduced with permission from Ref. [35]. Copyright © 2015 American Chemical Society

6.3.4 Conclusions and Future Outlook

The employment of micro- and nanomotors for medical treatment and diagnostics, chemotaxis, electronic repair, and environmental remediation has been realized. A wide array of machines has been created and their interactions with various chemical and external fields have been studied. While each propulsion system has their benefits and detriments, careful pairing of particle size, morphology and composition with the input energy route can lead to machines that are highly efficient for the job they are employed to do. It is hopeful that in the future, nanomotors are created with an enhanced ability to work in complex sample matrices and ability to move in biologically and environmentally relevant fuel concentrations.

References

1. Badjić, J.D., et al. 2004. A molecular elevator. *Science* 303: 1845–1849.
2. Bruns, C.J., and J.F. Stoddart. 2014. Rotaxane-based molecular muscles. *Accounts of Chemical Research* 47: 2186–2199.
3. Balzani, V., et al. 2006. Autonomous artificial nanomotor powered by sunlight. *Proceedings of the National Academy of Sciences* 103 (5): 1178–1183.
4. Duan, W., et al. 2015. Synthetic nano- and micromachines in analytical chemistry: Sensing, migration, capture, delivery and separation. *Annual Review of Analytical Chemistry* 8: 311–333.
5. Ge, Y., et al. 2016. Dual-fuel-driven bactericidal micromotor. *Nano-Micro Letters* 8 (2): 157–164.
6. Li, J., et al. 2015. Self-propelled nanomotors autonomously seek and repair cracks. *Nano Letters* 15: 7077–7085.
7. Kagan, D., P. Calvo-Marzal, S. Balasubramanian, S. Sattayasamitsathit, K.M. Manesh, G. Flechsig, and J. Wang. 2009. Chemical sensing based on catalytic nanomotors: Motion-based detection of trace silver. *Journal of the American Chemical Society* 131: 12082–12083.
8. Demirok, U.K., et al. 2008. Ultrafast catalytic alloy nanomotors. *Angewandte Chemie International Edition* 47 (48): 9349–9351.
9. Cai, K., et al. 2016. A method for measuring rotation of a thermal carbon nanomotor using centrifugal effect. *Scientific Reports* 6: 27338.
10. Wang, W., et al. 2013. Understanding the efficiency of autonomous nano- and microscale motors. *Journal of the American Chemical Society* 135: 10557–10565.
11. Liu, R., and A. Sen. 2011. Autonomous nanomotor based on copper-platinum segmented nanobattery. *Journal of the American Chemical Society* 133: 20064–20067.
12. Vach, P.J., S. Klumpp, and D. Faivre. 2016. Steering magnetic micropropllers along independent trajectories. *Journal of Physics D: Applied Physics* 49: 065003.
13. Gao, W., et al. 2012. Cargo-towing fuel-free magnetic nanowsimmers for targeted drug delivery. *Small* 8 (3): 460–467.
14. Chen, J., et al. 2015. Impeded mass transportation due to defects in thermally driven nanotube nanmotor. *Journal of Physical Chemistry C* 119: 17362–17368.
15. Li, J., et al. 2014. Water-driven micromotors for rapid photocatalytic degradation of biological and chemical warfare agents. *ACS Nano* 8: 11118–11125.

16. Abdelmohsen, L.K.E.A., M. Nijemeisland, G.M. Pawar, G.A. Janssen, R.J.M. Nolte, J.C.M. van Hest, and D.A. Wilson. 2016. Dynamic loading and unloading of proteins in polymeric stomatocytes: Formation of an enzyme-loaded supramolecular nanomotor. *ACS Nano* 10: 2652–2660.
17. Gao, W., S. Sattayasamitsathit, and J. Wang. 2012. Catalytically propelled micro-/nanomotors: How fast can they move? *The Chemical Record* 12 (1): 224–231.
18. Young, L.E. 2009. Equine athletes, the equine athlete's heart and racing success. *Experimental Physiology* 88 (5): 659–663.
19. Rubin, S., M.H. Young, J.C. Wright, D.L. Whitaker, and A.N. Ahn. 2016. Exceptional running and turning performance in a mite. *Journal of Experimental Biology* 219: 676–685.
20. Bustamante, C., D. Keller, and G. Oster. 2001. The physics of molecular motors. *Accounts of Chemical Research* 34: 412–420.
21. Roberts, A.J., et al. 2013. Functions and mechanisms of dynein motor proteins. *Nature Reviews Molecular Cell Biology* 14: 713–726.
22. Bayly, P.V., and S.K. Dutcher. 2016. Steady dynein forces induce flutter instability and propagating waves in mathematical models of flagella. *Journal of the Royal Society, Interface* 13 (123): 20160523.
23. Gennerich, A., and R.D. Vale. 2009. Walking the walk: How kinesin and dynein coordinate their steps. *Current Opinion in Cell Biology* 21: 59–67.
24. Ishijima, S. 2016. Self-sustained oscillatory sliding movement of doublet microtubules and flagellar bend formation. *PLoS ONE* 11 (2): e0148880.
25. Esteban-Fernández de Ávila, B., et al. 2016. *Acoustically propelled nanomotors for intracellular siRNA delivery. ACS Nano*. **10**: p 4997–5005.
26. Purcell, E.M. 1977. Life at low reynolds number. *American Journal of Physics* 45: 3–11.
27. Wang, W., et al. 2015. From one to many: Dynamic assembly and collective behavior of self-propelled colloidal motors. *Accounts of Chemical Research* 48: 1938–1946.
28. Pavlick, R.A., et al. 2011. A polymerization-powered motor. *Angewandte Chemie International Edition* 50 (40): 9374–9377.
29. Ma, X., et al. 2015. Enzyme-powered hollow mesoporous janus nanomotors. *Nano Letters* 15: 7043–7050.
30. Wong, F., and A. Sen. 2016. Progress toward light-harvesting self-electrophoretic motors: Highly efficient bimetallic nanomotors and micropumps in halogen media. *ACS Nano* 10: 7172–7179.
31. Perro, A., et al. 2009. Production of large quantities of "Janus" nanoparticles using wax-in-water emulsions. *Colloids and Surfaces A* 332 (1): 57–62.
32. Walker, D., et al. 2015. Optimal length of low reynolds number nanopropellers. *Nano Letters* 15 (7): 4412–4416.
33. Mandal, P., V. Choptra, and A. Ghosh. 2015. Independent positioning of magnetic nanomotors. *ACS Nano* 9 (5): 4717–4725.
34. Gao, W., et al. 2011. Hybrid nanomotor: A catalytically/magnetically powered adaptive nanowire swimmer. *Small* 7 (14): 2047–2051.
35. Li, J., et al. 2015. Magneto-acoustic hybrid nanomotor. *Nano Letters* 15: 4814–4821.
36. Wang, W., et al. 2015. A tale of two forces: Simultaneous chemical and acoustic propulsion of bimetallic micromotors. *Chemical Communications* 51: 1020–1023.
37. Ahmed, S., et al. 2016. Density and shape effects in the acoustic propulsion of bimetallic nanorod motors. *ACS Nano* 10: 4763–4769.
38. Wang, W., et al. 2012. Autonomous motion of metallic microrods propelled by ultrasound. *ACS Nano* 6: 6122–6132.
39. Nadal, F., and E. Lauga. 2014. Asymmetric steady streaming as a mechanism for acoustic propulsion of rigid bodies. *Physics of Fluids* 26: 082001.
40. Rao, K.J., et al. 2015. A force to be reckoned with: A review of synthetic microswimmers powered by ultrasound. *Small* 11 (24): 2836–2846.
41. Liaw, J., Y. Chen, and M. Kuo. 2014. Rotating Au nanorod and nanowire driven by circularly polarized light. *Optics Express* 22 (21): 26005–26015.

42. Liaw, J., Y. Chen, and M. Kuo. 2016. Spinning gold nanoparticles driven by circularly polarized light. *Journal of Quantitative Spectroscopy and Radiative Transfer* 175: 46–53.
43. Guix, M., C.C. Mayorga-Martinez, and A. Merkoçi. 2014. Nano/micromotors in (bio) chemical science applications. *Chemical Reviews* 114: 6285–6322.
44. Bonin, K.D., B. Kourmanov, and T.G. Walker. 2002. Light torque nanocontrol, nanomotors and nanorockets. *Optics Express* 10 (19): 984–989.
45. Sundararajan, S., et al. 2008. Catalytic motors for transport of colloidal cargo. *Nano Letters* 8: 1271–1276.
46. Lee, Y., and Z. Wu. 2015. Enhancing macrophage drug delivery efficiency via co-localization of cells and drug-loaded microcarriers in a 3D resonant ultrasound field. *PLoS ONE* 10 (8): e0135321.
47. Pijper, D., et al. 2005. Acceleration of a nanomotor: Electronic control of the rotary speed of a light-driven molecular rotor. *Journal of the American Chemical Society* 127 (50): 17612–17613.
48. Eelkema, R., et al. 2006. Nanomotor rotates microscale objects. *Nature* 440: 163.
49. Chałupniak, A., E. Morales-Narváez, and A. Merkoçi. 2015. Micro and nanomotors in diagnostics. *Advanced Drug Delivery Reviews* 95: 104–116.
50. Küchler, A., et al. 2016. Enzymatic reactions in confined environments. *Nature Nanotechnology* 11: 409–420.
51. Akhavan, O., M. Saadati, and M. Jannesari. 2016. Graphene jet nanomotors in remote controllable self-propulsion swimmers in pure water. *Nano Letters* 15: 5619–5630.